Environmental Toxicology and Pharmacology 110 (2024) 104503

Contents lists available at ScienceDirect

Environmental Toxicology and Pharmacology

journal homepage: www.elsevier.com/locate/etap

The porcine corpus luteum as a model for studying the effects of nanoplastics

Giuseppina Basini [a,*], Simone Bertini [a], Simona Bussolati [a], Francesca Zappavigna [a], Melissa Berni [b], Erika Scaltriti [b], Roberto Ramoni [a], Stefano Grolli [a], Fausto Quintavalla [a], Francesca Grasselli [a]

[a] *Dipartimento di Scienze Medico-Veterinarie, Università degli Studi di Parma, Via del Taglio 10, Parma 43126, Italy*
[b] *Risk Analysis and Genomic Epidemiology Unit, Istituto Zooprofilattico Sperimentale della Lombardia e dell'Emilia Romagna, Strada dei Mercati 13a, Parma 43126, Italy*

ARTICLE INFO

Keywords:
Ovary
Luteal cells, endothelial cells
Plastic
ROS
VEGF
Progesterone

ABSTRACT

Nanoplastics (NPs) affect fertility. We evaluated the effects of NPs treatment on luteal and endothelial cells. We examined crucial markers of growth and redox status. NPs treatment did not induce changes in ATP levels in luteal cells, while it increased ($p< 0.05$) their proliferation. In endothelial cells, no change in proliferation was detected, while an increase ($p<0.05$) in ATP levels was observed. The increase of reactive oxygen species, superoxide anion ($p<0.05$) and nitric oxide ($p<0.001$) was detected in both cell types, which also showed changes in superoxide dismutase enzyme activity as well as an increase of non-enzymatic antioxidant power ($p<0.05$). A decrease ($p<0.05$) in progesterone production as well as an increase of vascular endothelial growth factor A levels were detected ($p<0.05$). In addition, a dose-dependent accumulation of NPs in endothelial cells was shown, that likely occurred through adhesion and internalization. Results underline potential risk of NPs for corpus luteum functionality.

1. Introduction

The word "plastic" comes from the ancient Greek word "plastikos", which means "able to assume various shapes" (Sangale et al., 2019). Plastics are synthetic polymers composed by chains of carbons, surrounded by hydrogen, oxygen, nitrogen, and sulphur which are used worldwide. They have gradually replaced other materials such as wood, metal, and glass in a variety of applications due to their low cost, durability and high strength. Plastics are broadly utilized in industrial applications as well as in everyday life products (Ali et al., 2021). Global plastic production is reported to have reached 400.3 million tons in 2022 and, due to their robust environmental stability, plastic products are now as ubiquitous as they are persistent. Unfortunately, less than 9 % of plastic is recycled and plastic pollution represents a major current environmental problem (PlasticsEurope, 2023). In addition to an increasingly evident accumulation of plastic waste, one of the most critical novel aspects related to pollution is the formation of fragments due to the action of chemical and physical agents. Microplastics (MPs) size ranges from 1 µm to 5 mm while nanoplastics (NPs) are particles smaller than 100 nm; their presence has been detected in the environment (Sridharan et al., 2021; Athulya et al., 2024; Liza et al., 2024), in food (Ferreira et al., 2023; Milne et al., 2024), drinks (Sewwandi et al., 2023) as well as in living organisms (Malafeev et al., 2023). Animals and humans can encounter MPs and NPs through ingestion, breathing and trans dermally (Jeong et al., 2024). Furthermore, given their small size, recent evidence suggests that nanoplastics can overcome biological barriers, being able to penetrate organs and tissues and thus affecting physiological functionality of organs and tissues (Khan and Jia, 2023). Therefore, the broader Anthropocene Epoch also includes the Plasticene Era, where humans and animals are subjected pervasively to nano- and microplastics. A particular concern arises from potential effects on endocrine function (Leso et al., 2023), resulting in impairment of fertility (Hong et al., 2023). Therefore, in order to gain a deeper insight on this issue, the aim of the present study was to evaluate the effects of NPs on reproductive functionality, by studying the effects of 100 nm polystyrene NPs at three different concentrations (5, 25 and 75 µg/mL) (Basini et al., 2021a, 2022, 2023). Swine corpus luteum, a transient endocrine organ mainly composed by steroidogenic and endothelial cell

* Corresponding author.
E-mail address: basini@unipr.it (G. Basini).

https://doi.org/10.1016/j.etap.2024.104503
Received 31 May 2024; Received in revised form 10 July 2024; Accepted 14 July 2024
Available online 24 July 2024

(Dodi et al., 2021), was chosen as experimental model. We examined the main cellular functionality parameters of sow luteal cell cultures, used as a model of endocrine reproductive cells (Basini et al., 2018a, 2021b; Dodi et al., 2021), and of porcine endothelial cells (Basini et al., 2014) used as a model for evaluating the angiogenesis process, fundamental in formation and maintenance of the corpus luteum. On both cell types, we considered potential effects on cell growth, measuring BrdU uptake, as a marker of cell proliferation and ATP production, as indicator of metabolic activity. Since redox balance is a key area of physiological cell function, we tested NPs effect on oxidative stress markers, considering superoxide anion (O_2^-) as reactive oxygen species and nitric oxide (NO) as reactive nitrogen species examples. Moreover, we also tested the potential effects of NO on antioxidant defence mechanisms, considering both enzymatic (superoxide dismutase activity, SOD) and non-enzymatic (Ferric Reducing Activity of Plasma, FRAP) ones. As specific cellular markers, the synthesis of progesterone (P4) ad vascular endothelial factor A (VEGF) as crucial hallmarks of luteal and endothelial cell function respectively were measured. In arterial and venous endothelial cells, the accumulation of NPs has been already observed and linked to adverse effects *in vitro*, like induction of oxidative stress, alteration of VEGF production, damaging of cytoskeletal junctions and to the related consequences on the cardiovascular system *in vivo* (Shiwakoti et al., 2022; Wei et al., 2022 Basini et al., 2023; Lee et al., 2024). Whereas less is known about the consequences of NPs exposure on microvascular endothelial cells specific of the ovary, even if the ovarian functionality is strictly dependent on the establishment and continual remodelling of the microvascular system (Robinson et al., 2009). Furthermore, in recent *in vivo* and *in vitro* studies, NPs were already reported to accumulate in ovarian endocrine cells (Huang et al., 2022; Zeng et al., 2023), while, to our knowledge, no investigations were performed on NPs accumulation in ovarian endothelial cells. Thus, in addition to the evaluation of the effects of NPs exposure on reproductive functionality in sow luteal and endothelial cells, we aim to investigate the occurrence of NPs accumulation in the latter isolated from sow corpus luteum, proposed here as a model of a reproductive organ.

2. Materials and methods

All reagents used in this study were obtained from Merck (Darmstadt, Germany) unless otherwise specified.

2.1. Isolation and culture of luteal and endothelial cells from swine corpus luteum cells

We collected ovaries from Large White cross-bred gilts, parity=0 at a local abbattoir. On the basis of previous observations (Akins and Morrissette, 1968; McDonald, 1975; Babalola and Shapiro, 1988; Gregoraszczuk and Oblonczyk, 1996; Nitkiewicz et al., 2010) the stage of the estrous cycle was determined by evaluating ovarian morphology. In particular, 20 animals were chosen and their ovaries, presumably in the luteal phase, were carried to the lab within 1 hour into sterile phosphate-buffered saline (PBS, 4°C) containing 500 IU/mL penicillin, 500 μg/mL streptomycin and amphotericin B (3.5 μg/mL) (Basini et al., 2010, 2017, 2018a). The ovaries were then cleaned for 1 min in ethanol 70 % and washed with sterile PBS. Luteal tissue was collected from pools of freshly excised corpora lutea of ten animals in mid luteal phase and then it was enzymatically dissociated as described by Gospodarowicz and Gospodarowicz (1972). Thereafter, we proceeded to corpora lutea mincing and enzymatic dissociation of corpora lutea in PBS added with BSA (1 mg/mL), collagenase type-I e II (1 mg/mL; Gibco, Waltham, MA) and DNAse (1 mg/mL) for 1 hour at 37°C in a shaker water bath (Basini et al., 2018). Afterwards, cells were filtered through a 40 μm filter and subjected to a 1 min treatment with ammonium chloride 0.17 M at 37°C to remove red blood cells. Cells were then centrifuged at 300 x g for 10 min. Vital staining with trypan blue dye (0.4 % w/v) was used to determine cell viability. Consistent with fine structural analyses, the large luteal cells isolated from various nonprimate species measure ≥ 20 μm while small luteal cells < 20 μm (Leung and Adashi, 2018). Therefore, the filtration in our protocol is useful to block cell debris while large luteal cells can pass the mesh and our cell population is a mix of small and large luteal cells.

Luteal cells were then seeded at different densities into 96-well plates containing 200 μL M199 culture medium added with sodium bicarbonate (2.2 mg/mL), penicillin (100 UI/mL), streptomycin (100 μg/mL), amphotericin B (2.5 mg/mL) and 10 % foetal bovine serum (FBS) (Basini et al., 2018).

Endothelial cells were isolated from swine ovaries collected as above described (Spanel-Borowski and van der Bosch, 1990). The modified protocol and cell characterization have been described in our previous study (Basini et al., 2014). The last cell suspension obtained was firstly filtered with a sterile gauze (150 mesh) and then by a 70 μm filter (BD Falcon, Bedford Bioscience, USA). To eliminate the red blood cells, we treated cell suspension with 0.17 M NH_4Cl for 1 min and centrifuged at 500 x g for 10 min. After achieving isolation, 500 μL of cell suspension were put in 25 cm^2 flasks with 5 mL EBM-2 plus EGM-2 (Clonetics, Lonza, Walkersville, MD USA); every 48 h, culture medium was changed thus eliminating not adherent cells.

Both luteal and endothelial cells were subjected to a 48 h incubation carried out at 37°C, 5 % CO_2, and 95 % humidified air, with or without polystyrene NPs at the concentrations of 5, 25 and 75 μg/mL (Lehner et al., 2019; Shen et al., 2019; Basini et al., 2021a, 2022, 2023) (Sigma Aldrich catalogue N. 43302). The particles, with a mean diameter of100 nm, were in aqueous suspension (10 % WT) with a density of 1.05 g/cm^3.

2.2. Cell proliferation

Luteal and endothelial cell proliferation were evaluated by BrdU incorporation assay test (Roche Diagnostics, Mannheim, Germany. Briefly, 10^4 luteal cells/well and 1.5×10^3 endothelial cells/200 μL medium were put in 96-well plates and incubated for 24 h at 37°C, 5 % CO_2, and 95 % humidified air. Medium was then removed, and cells were subjected to a 48 h treatment with 5, 25 and 75 μg/μL of NPs.as above detailed.

BrdU label (20 μL) was added to each well and incubated overnight. At the end, plates were centrifuged at 400 x g for 10 min, medium was removed, and we added a FixDenat Solution (200 μL) to favour antibody detection of the incorporated BrdU; in fact, wells were added with conjugated anti-BrdU antibody and detection of immune complexes was carried out by the subsequent substrate reaction. After stopping the reaction, the product was determined by measuring absorbance at a wavelength of 450 nm with Victor Nivo spectrophotometer (Perkin Elmer, Groningen, Netherland (Dodi et al., 2021).

2.3. Cell metabolic activity

2×10^5 viable luteal cell and 5×10^4 endothelial cells /200 μL medium were seeded in 96-well plates added with NPs for 48 h as described above. A bioluminescent assay (ATP-lite 1-step; Perkin Elmer, Groningen, Netherlands) which quantifies intracellular ATP levels was employed to assess cell metabolic activity. ATP, which is present in all metabolically active cells, represents is a viability marker whose levels rapidly decrease during cell necrosis or apoptosis. The ATP lite-1 step assay system relies on the detection of light resulting from the reaction of ATP with D-luciferin catalysed by luciferase. The emitted light is proportional to the ATP concentration. Briefly, 100 μL of cell suspension were added with 100 μL of substrate solution and the luminescence was quantified by Victor Nivo (Basini et al., 2021b).

2.4. Cell redox status

2.4.1. Non-enzymatic scavenging activity

The ability of antioxidants in biological samples to reduce ferric-tripiridyltriazine (Fe^{3+} TPTZ) to a ferrous form (Fe^{2+} TPTZ) can be assessed by using the colorimetric method known as The Ferric Reducing Ability of Plasma (FRAP) assay. Before use we prepared the TPTZ reagent by mixing 25 mL of acetate buffer, 2.5 mL of 2,4,6-Tris(2-pyridyl)-s-triazine (TPTZ) 10 mM in HCl 40 mM and $FeCl_3$–6 H_2O solution. Seedings of 2×10^5 luteal cells/well and 5×10^4 viable endothelial cells were carried out in 96-well plates and cells were subjected to a 48 h treatment with NPs as described above (37°C, 5 % CO_2, and 95 % humidified air). Thereafter, plates were centrifuged at 400 x g for 10 min, supernatants were discarded, and lysis was obtained immersing cells in ice bath for 30 min, with cold Triton 0.5 % + PMSF in PBS (200 μL/well). 40 μL of cell lysates were added to Fe^{3+} TPTZ reagent and incubated at 37°C for 30 min. The reduction developed a blue colour that was read by Victor Reader at 595 nm. The reducing ability was determined using a standard curve of absorbance against $FeSO_4$-7 H_2O standard solution (Dodi et al., 2021).

2.4.2. Enzimatic scavenging activity: superoxide dismutase (SOD)

SOD Assay Kit was used to determine SOD activity. Cell culture (2×10^5 luteal cells and 5×10^4 endothelial cells) was carried out for 48 h in 96-well plates (Sarstedt, Nümbrecht, Germany) added with NPs as described above. Cells were centrifuged for 10 min. at 400 × g, the supernatants were discarded, and cell lysis was obtained as above specified. Cell lysates were assessed without dilution and a standard curve of SOD ranging from 0.156 to 20 U/mL was prepared. The assay measured formazan produced by the reaction between a tetrazolium salt and a superoxide anion (O_2^-), resulting from the reaction of an exogenous xantine oxidase. The endogenous SOD activity is indirectly evalutated by assessing the remaining O_2^-. Determination of the absorbance was carried out with Victor Nivo reading at 450 nm against 620 nm (Basini et al., 2024).

2.4.3. Nitric oxide (NO) production

Cell seeding (10^5 luteal cells/well and 5×10^4 endothelial cells) was carried out for 48 h in 96-well plates (37°C, 5 % CO_2, and 95 % humidified air) in the presence of NPs as above detailed. Plates were then centrifuged for 10 min at 400 x g and supernatants were collected. NO production was assessed by Griess test which quantifies nitrite levels in supernatants of cultured cells (Basini et al., 2009a, 2014, 2018).

2.4.4. Superoxide (O_2^-) production

O_2^- produced by cultured cells was determined by Cell-Proliferation Reagent WST-1 test (Roche Diagnostics, Indianapolis, In, USA) (Basini et al., 2009b, 2017). 10^4 luteal cells/well and 1.5×10^3 endothelial cells were cultured in 96-well plates for 48 h (37°C, 5 % CO_2, and 95 % humidified air) in the presence of NPs at the concentrations indicated above. After the addition of 20 μL WST-1during the last 4 h of incubation, absorbance was determined using Victor Nivo at a wavelength of 450 nm against 620 nm (Basini et al., 2021b).

2.5. Luteal cell progesterone (P4) production

Progesterone ELISA (DiaMetra, Boldon, UK) is a competitive immunoenzymatic colorimetric assay for assessing P4 levels. After seeding of 10^4 cells /well) in 96-well plates incubation was carried out with NPs as above indicated for 48 h (37°C, 5 % CO_2, and 95 % humidified air). Plates were then centrifuged at 400 x g for 10 min and supernatants were collected, frozen and stored at −20°C until P4 quantification. We added 200 μL of antigenic progesterone conjugated with horseradish peroxidase (HRP) to 20 μL of samples in a microplate coated with antibodies anti-progesterone. The reaction with Substrate (H_2O_2) and TMB Substrate was catalysed by the enzyme in the bound fraction. The reaction colour changed from blue to yellow after the addition of Stop Solution (H_2SO_4). P4 levels, inversely proportional to the developed colour intensity, was quantified by using Victor reader at a wavelength of 450 nm through a calibration curve (Dodi et al., 2021).

2.6. Endothelial cell VEGF production

The ELISA test (Quantikine, R&D System, Minneapolis, MI, USA), validated for pig VEGF (Barboni et al., 2000; Basini et al., 2023) allows VEGF A levels determination in spent media. The assay sensitivity was 0, 23 0.23 pmol/L, and the intra- and inter-assay CVs were always less than 7 %. We seeded 1×10^5 cells (500 μL CM) in 24-well plates and cultured them for 24 h at 37 ∘C in humidified atmosphere (5 % CO_2) for 24 h. After media removal, a 48 h treatment with NPs was carried out.

2.7. Study of NPs accumulation in endothelial cells through fluorescence microscopy

2.7.1. Assessment of the NPs load in endothelial cells

Endothelial cell seeding (3×10^3 cells/well) was carried out in 96 well plates for fluorescence imaging (Cellvis, Mountain View, CA) 20–24 hours before the assay. Then, endothelial cell monolayers were treated for 48 hours with fluorescent polystyrene NPs of 100 nm of diameter (Sigma Aldrich, catalogue N. L9940) at 5, 25 and 75 μg/μL. The same time of exposure and concentrations of NPs were tested in recent observations (Basini et al., 2023). Furthermore, the range of concentrations examined is consistent with the accumulation of NPs reported in tissues of experimental animals following *in vivo* exposure (Dong et al., 2023). After 48 h of NPs treatment, samples were fixed with paraformaldehyde 4 % in PBS. For the quantification of the NPs load, the fixed samples were permeabilized for 15 min with triton 0,1X in PBS. Then, endothelial cells were marked by labelling F-actin with Phalloidin-Alexa Fluor 647 (Invitrogen) and nuclei were stained with DAPI (Invitrogen) following manufacturer's instruction. Labelled F-actin (Ex/Em 650/671 nm), nuclei (Ex/Em 346/442 nm) and fluorescent NPs (Ex/Em 475/540 nm) were imaged with the motorized Axio Observer Inverted Fluorescence Microscope, equipped with Colibrì 5/7 LED Light Source, using Axiocam 305 mono and ZEN 3.1 blue software (ZEISS). For each technical replicate, 2–4 random fields were acquired using a 20x/0.8 NA objective. The image analysis was performed using ImageJ software (Schindelin et al., 2012). To quantify the NPs load in endothelial cells, the image analysis described in our previous study was used (Basini et al., 2023), that was a modification of the "Area Analysis" by Berni and collegues (Berni et al., 2022). Briefly, NPs and F-actin channels were split and processed separately. Then, a threshold was set for each channel in order to exclude the background from the area measurement. Since a Z-stack was acquired, the threshold was set on the Maximum Intensity Projection (MIP) of the Z-stack. Finally, for each image acquired the area occupied by pixels corresponding to NPS and endothelial cells (F-actin) was measured. The ratio (NPs Area/-Endothelial Cells Area) was then calculated to have a quantitative measurement of the NPs load in treated monolayers. For each technical replicate, the sum of the endothelial cell areas and of the NPs areas of all the fields acquired was used to calculate the ratio.

2.7.2. Investigation of NPs internalization in endothelial cells

To investigate the possible internalization of NPs in endothelial cells, we verified if NPs co-localized with cytosolic lysosomes, that was previously reported in different cell types (Khan et al., 2023; Brandts et al., 2023; Huang et al., 2023). For this purpose, endothelial cells were treated with 5 μg/mL of fluorescent NPs as described above with some modifications. First, the lysosomal marker LAMP-1 was labelled in fixed and permeabilized samples. Briefly, samples were blocked for 1 hour in bovine serum albumin (BSA) 1 % in PBS, then incubated at room temperature for 3 hours with 1 mg/mL of Anti-LAMP-1 primary antibody (CD107a clone 4E9/11, Invitrogen) in blocking solution. Then, samples were incubated with 1 mg/mL of Goat anti-Mouse IgG secondary antibody conjugated with Alexa Fluor 647 (Invitrogen) in BSA 0,2 % in PBS. Finally, samples were imaged as described above, but using the Apotome 3 for the optical sectioning in fluorescence imaging (ZEISS). A 6,37 µm Z-stack was acquired (13 slices with a 0,49 µm interval) using Alexa Fluor 647 as reference channel for the software autofocus. Orthogonal x, z and y,z projections and Depth-coding 3D reconstructions were produced using ZEN 3.1 blue software (ZEISS) to investigate co-localization between lysosomes and NPs.

2.8. Statistical analysis

The experiments were repeated at least five times with six replicates for each treatment. Data are presented as mean ± SEM (standard error of mean). Statistical difference was calculated by One-Way ANOVA using Statgraphics software (STC Inc., Rockville, MD, USA). In the presence of a significant difference ($p<0.05$), the means were subjected to Scheffé F test for multiple comparisons.

3. Results

3.1. Luteal cell growth

The metabolic activity of the luteal cells, assessed through the quantification of ATP production, was not affected by the presence of NPs at any concentration used for the 48 h incubation (Fig. 1 A). Luteal cell proliferation, estimated by BrdU incorporation into newly synthesized DNA, was significantly stimulated ($p<0.05$) by the three dosages tested, without significant differences between them ($p<0.05$) (Fig. 1 B).

3.2. Luteal cell P4 production

Progesterone production was found to be significantly inhibited ($p<0.05$) by all concentrations of NPs (5, 25, 75 µg/mL), without significant difference among those examined (Fig. 2).

3.3. Luteal cell redox status

In luteal cells, superoxide anion production was significantly stimulated ($p<0.05$) by NPs only by the highest concentration (75 µg/mL). Lower concentrations of NPs did not show a significant difference compared to control (Fig. 3 A).

NO production in luteal cells was significantly stimulated ($p<0.001$) by NPs at a highest concentration (75 µg/mL), without significant differences in treatments with lower concentration (5, 25 µg/mL) (Fig. 3 B).

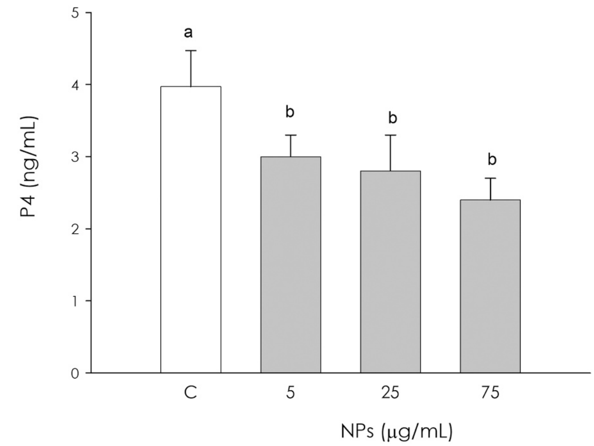

Fig. 2. Effect of the treatment with nanoplastics (NPs 5, 25 and 75 µg/mL) for 48 h on swine luteal cell progesterone production using ELISA assay. Data, expressed as ng/mL, represent the mean ± SEM of six replicates/treatment repeated in five different experiments. Different letters on the bars indicate a significant difference ($p < 0.05$) among treatments as calculated by ANOVA and Scheffè' F test.

NPs significantly inhibited ($p < 0.001$) the activity of the enzyme superoxide dismutase (SOD) in the luteal cells at all the concentrations tested, without significant differences among them ($p < 0.001$) (Fig. 3 C).

All concentrations of NPs (5, 25 and 75 µg/mL) exerted a significant ($p < 0.001$) increase of non-enzymatic antioxidant activity in luteal cells, without significant differences among the doses examined (Fig. 3 D).

3.3.1. Endothelial cell growth

The metabolic activity of endothelial cells from porcine corpus luteum, assessed by quantification of ATP production, was found to be significantly stimulated ($p<0.05$) by the presence of NPs at all the examined concentrations (Fig. 4 A).

Endothelial cell proliferation, assessed by BrdU incorporation into newly synthesized DNA was not significantly affected by any of the three concentrations examined (5, 25, 75 µg/mL) after 48 hours of incubation (Fig. 4 B).

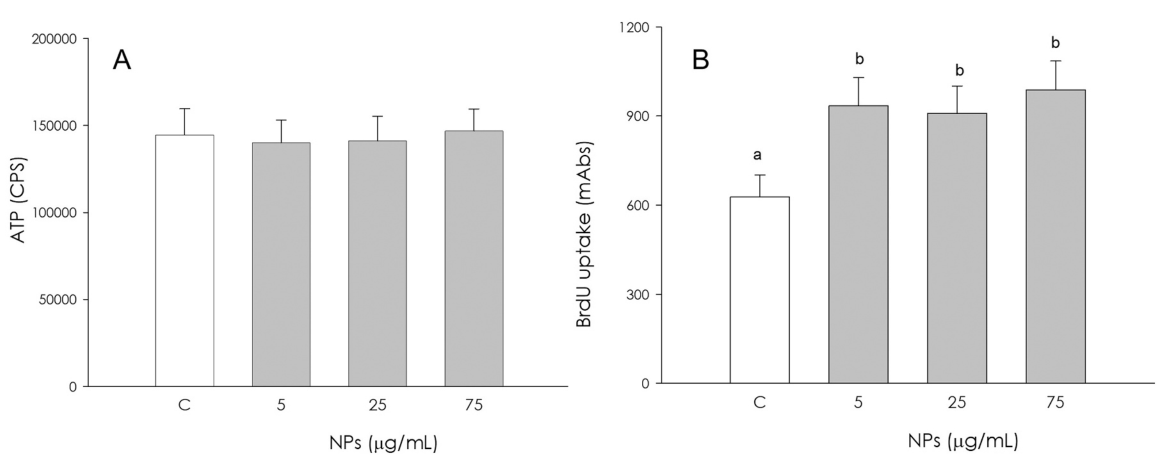

Fig. 1. Effect of the treatment with nanoplastics (NPs 5, 25 and 75 µg/mL) for 48 h on swine luteal cell metabolic activity using ATP content assay test (A) and proliferation using 5-bromo-2'-deoxyuridine (BrdU) incorporation assay test (B). Data, expressed as counts per second (CPS) in panel A and as milliabsorbance units (mAbs) in panel B, represent the mean ± SEM of six replicates/treatment repeated in five different experiments. Different letters on the bars indicate a significant difference ($p < 0.05$) among treatments as calculated by ANOVA and Scheffè' F test.

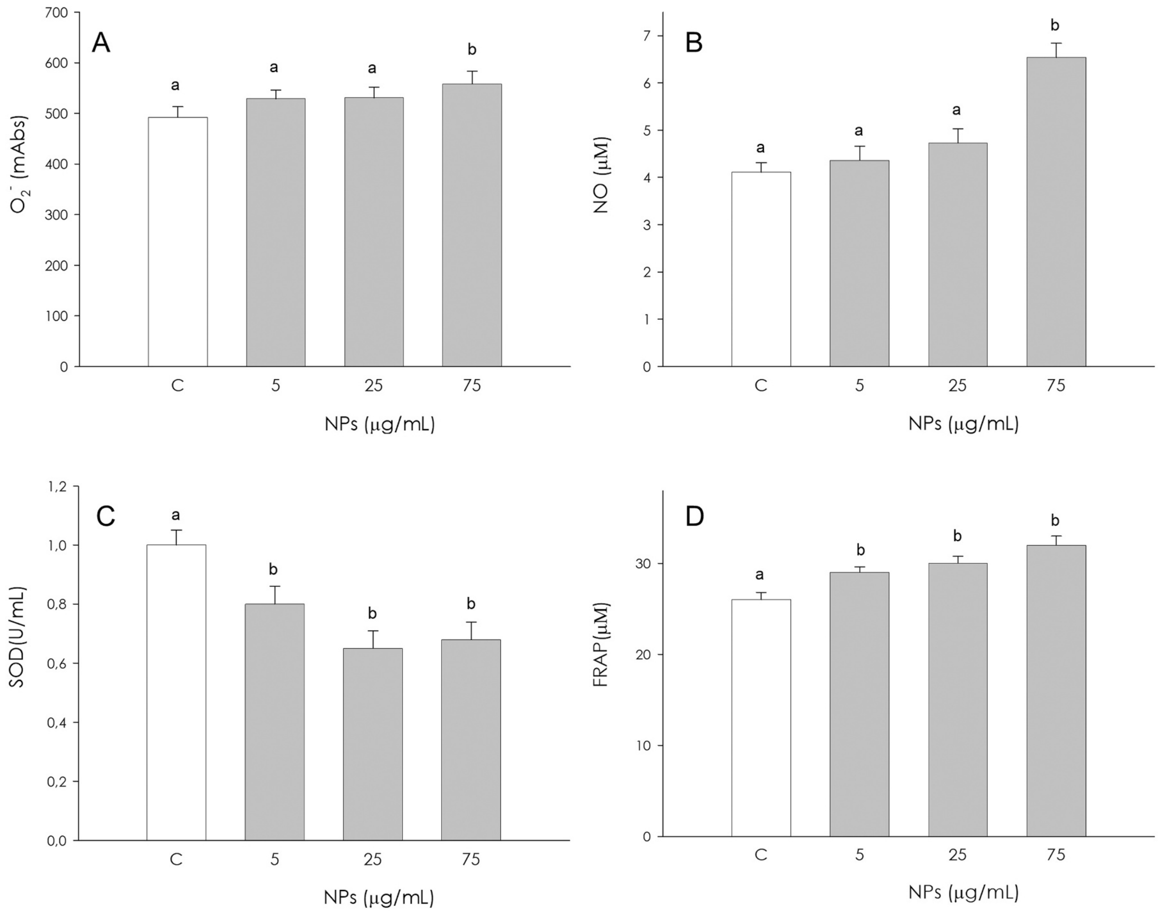

Fig. 3. Effect of the treatment with nanoplastics (NPs 5, 25 and 75 μg/mL) for 48 h on swine luteal cells superoxide anion (O_2^-) generation using colorimetric assay (A), nitric oxide (NO) production using Griess Assay (B), superoxide dismutase activity using SOD assay (C) and non-enzymatic scavenging activity using the FRAP assay (D). Data, expressed as milliAbs units (panel A), as μM (panel B and D), as U/mL (panel C), represent the mean ± SEM of six replicates/treatment repeated in five different experiments. Different letters on the bars indicate a significant difference ($p < 0.05$) among treatments as calculated by ANOVA and Scheffè' F test.

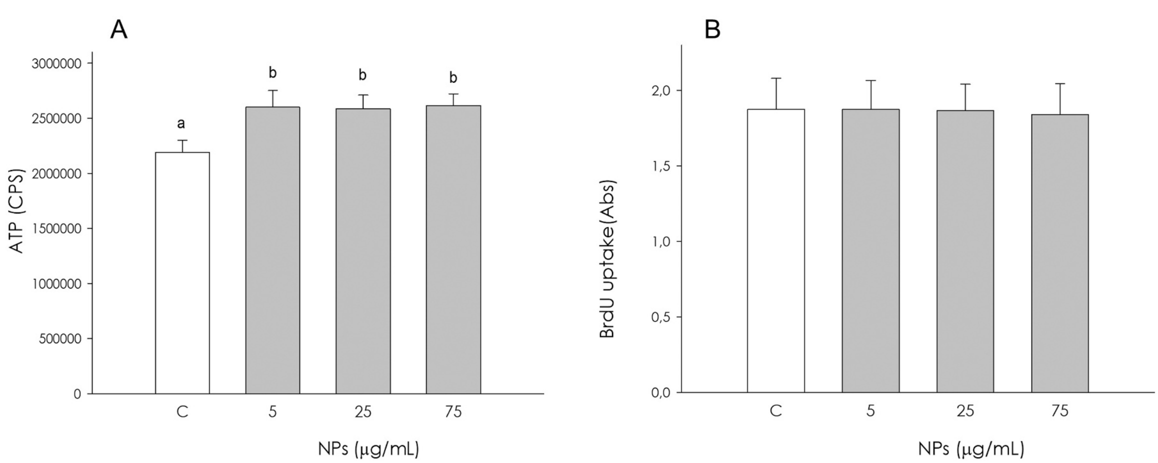

Fig. 4. Effect of the treatment with nanoplastics (NPs 5, 25 and 75 μg/mL) for 48 h on swine endothelial cell metabolic activity using ATP content assay test (A) and proliferation using 5-bromo-2'-deoxyuridine (BrdU) incorporation assay test (B). Data, expressed as counts per second (CPS) in panel A and as milliabsorbance units (mAbs) in panel B, represent the mean ± SEM of six replicates/treatment repeated in five different experiments. Different letters on the bars indicate a significant difference ($p < 0.05$) among treatments as calculated by ANOVA and Scheffè' F test.

3.3.2. Endothelial cell VEGF production

NPs significantly stimulated ($p < 0.05$) the production of VEGF by of porcine corpus luteum endothelial cells at all concentrations (Fig. 5).

3.3.3. Endothelial cell redox status

In endothelial cells the production of superoxide anion was significantly stimulated ($p<0.05$) by all concentrations NPs (Fig. 6 A).

NO production in endothelial cells was significantly ($p<0.001$) stimulated by NPs at concentrations of 25 and 75 μg/mL, with a greater

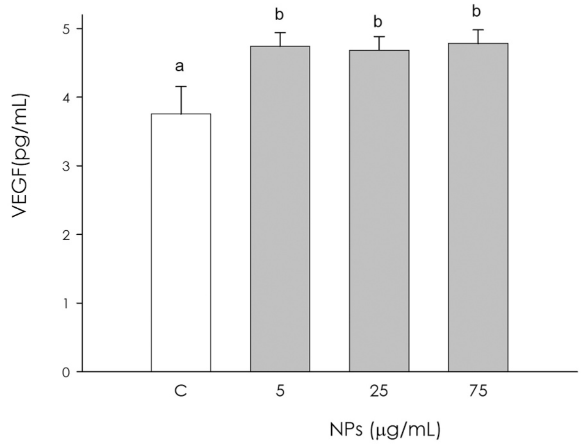

Fig. 5. Effect of the treatment with nanoplastics (NPs 5, 25 and 75 µg/mL) for 48 h on swine endothelial cells VEGF production using ELISA assay. Data, expressed as pg/mL, represent the mean ± SEM of six replicates/treatment repeated in five different experiments. Different letters on the bars indicate a significant difference ($p < 0.05$) among treatments as calculated by ANOVA and Scheffè' F test.

increase in the presence of the highest concentration (75 µg/mL) (Fig. 6 B).

NPs significantly stimulated ($p<0.05$) the enzymatic activity of superoxide dismutase (SOD) in endothelial cells without significant differences among the different doses examined ($p < 0.05$) (Fig. 6 C).

All three concentrations of NPs (5, 25, 75 µg/mL) exerted a significant stimulation ($p<0.05$) of non-enzymatic antioxidant activity in endothelial cells from swine corpus luteum (Fig. 6 D).

3.4. NPs accumulation in endothelial cells

3.4.1. NPs load in endothelial cells

The NPs load in endothelial cells was quantified through fluorescence microscopy image analysis and calculated as the (NPs Area/Endothelial Cell Area) ratio. Representative images of the treated monolayers (Fig. 7) clearly show that NPs were located in correspondence of fluorescently labelled F-actin and not randomly distributed. Data presented in Fig. 7 show that the NPs load was significantly higher at all the concentration tested as compared to the non-treated control. Then, a significant increase of the NPs load was observed not only between the lowest (5 µg/mL) and the other concentrations tested (25, 75 µg/mL), but also between the intermediate (25 µg/mL) and the highest (75 µg/mL) concentration tested. NPs accumulations wrapped around F-actin filaments were observed and reported through x,z and y,z orthogonal projections in Fig. S1.

3.4.2. NPs internalization in endothelial cells

The possibility of NPs internalization in endothelial cells was investigated using fluorescence microscopy by combining fluorescent NPs and fluorescent labelling of the lysosomal membrane protein LAMP-1. Specifically, the x,z and y,z orthogonal projections in Fig. 8 clearly show the presence of NPs accumulations (green) in between LAMP-1

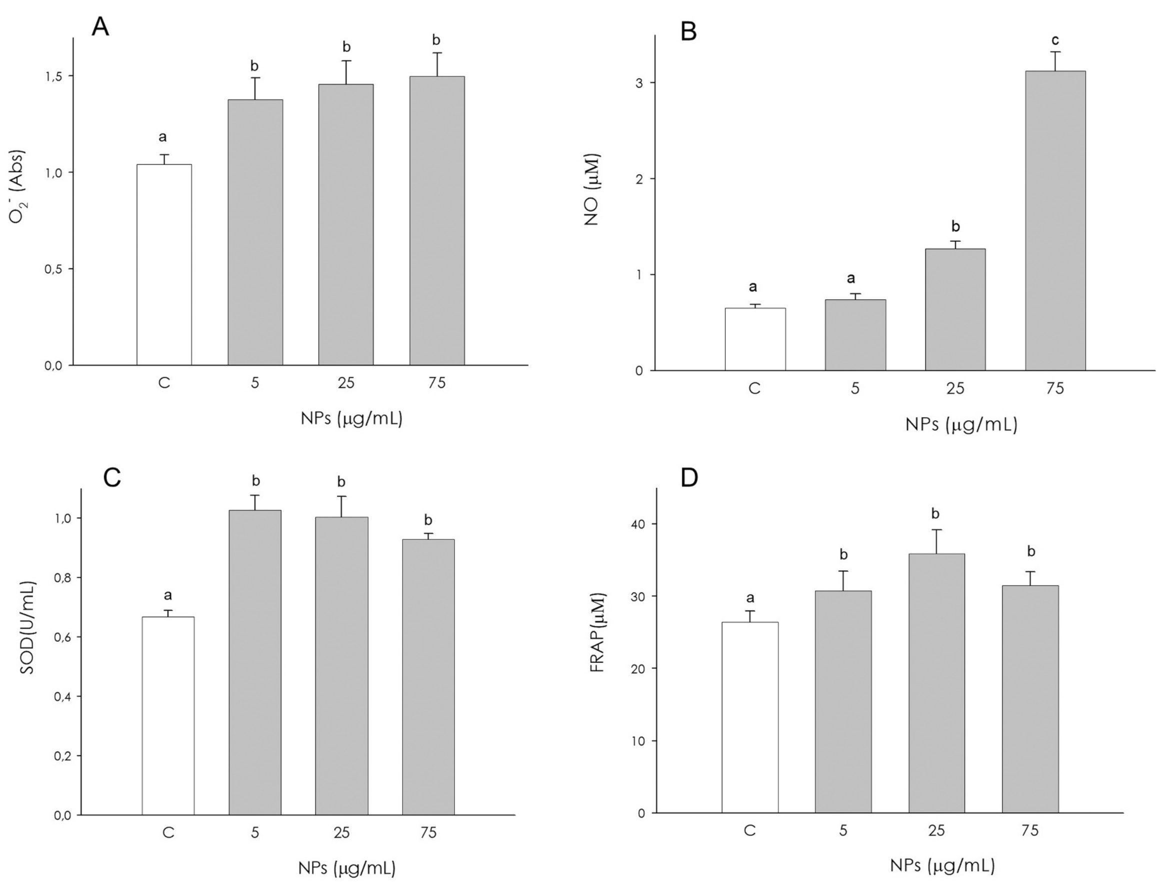

Fig. 6. Effect of the treatment with nanoplastics (NPs 5, 25 and 75 µg/mL) for 48 h on swine endothelial cells superoxide anion (O_2^-) generation using colorimetric assay (A), nitric oxide (NO) production using Griess Assay (B), superoxide dismutase activity using SOD assay (C) and non-enzymatic scavenging activity using the FRAP assay (D). Data, expressed as milliAbs units (panel A), as µM (panel B and D), as U/mL (panel C), represent the mean ± SEM of six replicates/treatment repeated in five different experiments. Different letters on the bars indicate a significant difference ($p < 0.05$) among treatments as calculated by ANOVA and Scheffè' F test.

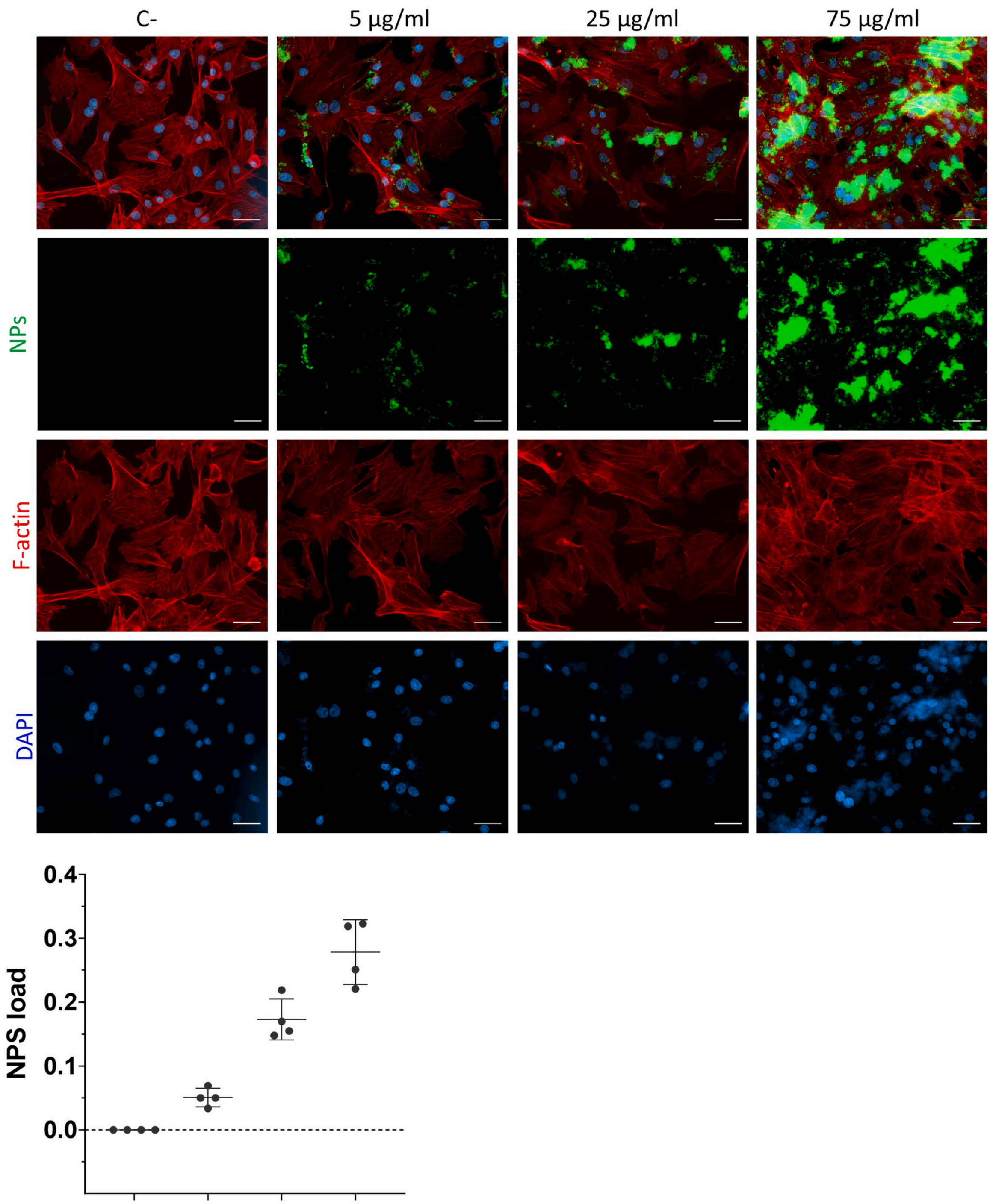

	C-	5	25	75
C-		3.99E-02	4.09E-04	8.62E-05
5			1.59E-03	1.56E-04
25				2.82E-03
75				

Fig. 7. Representative images of endothelial cells treated with different concentrations of NPs (negative control C-, 5, 25, 75 µg/mL). Endothelial cells are labeled in red (F-actin), nuclei in blue (DAPI) and NPs in green. White scale bars are 50 µm. The graph reports NPs load in endothelial cells, calculated as the (NPs Area/ Endothelial Cell Area) ratio. Each dot represents the ratio of a technical replicate. Means and standard deviation of the means were reported. p values obtained performing pairwise comparisons with One Way ANOVA with Tukey's correction were reported in the table below the graph.

positive lysosomes (red), demonstrating that NPs co-localized in z-dimension with cytosolic lysosomes. Depth-coding 3D reconstructions in Fig. 8 further confirmed the z-dimensional co-localization of LAMP-1 signal and NPs signal, thus intracellular localization of NPs. Otherwise, the inclusion of NPs into lysosomes was not confirmed since the complete overlapping of NPS signals with LAMP-1 signal was not observed. Furthermore, the accumulation of NPs that were not co-localized in z-dimension with lysosomes was also observed and reported through orthogonal projections in Fig. S2.

4. Discussion

Easy processing, versatility and low costs are among the most important characteristics attributable to plastic which justifies its use in multiple production contexts; in fact, today, plastic represents an essential material that is difficult to replace especially in the automotive industry and the building sector, such as with the formation of pipes, waterproofing and insulation. Its use is also widespread in the cosmetic sector since microplastics are added in exfoliating or cleansing products. With textiles, plastic is used in the manufacture of polyester garments. Furthermore, whilst disposable plastic packaging has contributed to food preservation, its role in the amount of discarded food waste has become a public issue in many countries. (Heidbreder et al., 2019). In addition, during the Sars-Cov-2 pandemic, the use of plastic polymers has grown exponentially in the medical healthcare sector, given the need to produce medical devices, diagnostic tools and disposable instruments to avoid virus transmission (Ekanayake et al., 2023). Unfortunately, due to the persistence of plastic and leaching from plastic waste in landfills, it is estimated that plastic pollution will have trebled from 2016 to 2040 unless appropriate measures are taken. A recent critical issue is associated with the various aging processes of plastics like mechanical abrasion, chemical oxidation, heat irradiation,

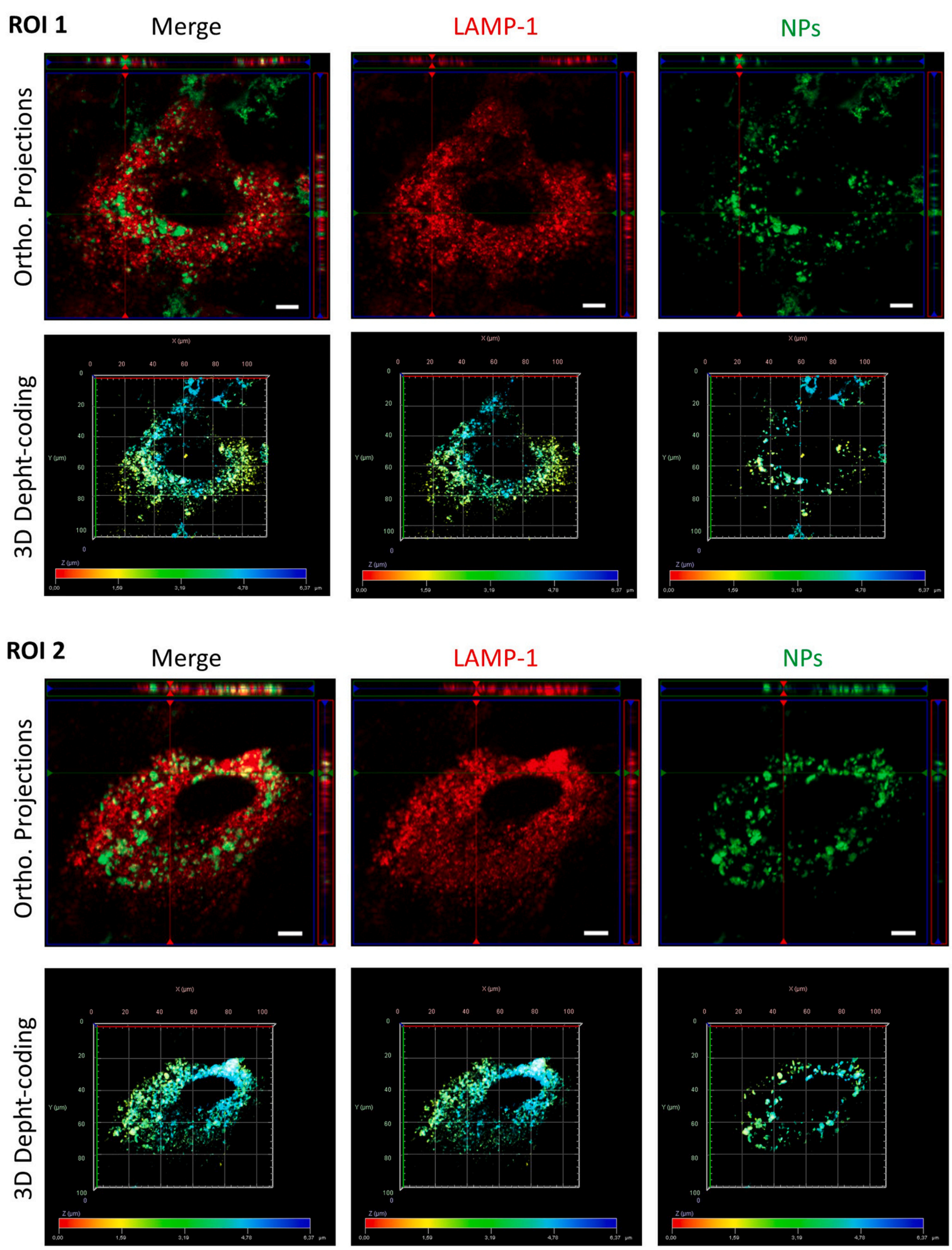

Fig. 8. NPs co-localization in z-dimension with lysosomes in endothelial cells treated with 5 μg/mL of NPs. In orthogonal projections the horizontal bars reconstruct x,z projection, while the vertical bars reconstruct the y,z projection. Lysosomes are shown in red (LAMP-1) and NPs in green. White scale bars are 10 μm. 3D Depht-coding reconstruction are reported with the legend color code.

biodegradation, ultraviolet (UV) irradiation, among others. In the environment, sunlight or UV radiation is considered to be the main cause of plastic aging, which likely induces chain scission and polymer chain reactions, leading to plastic fragmentation into particles (Junaid et al., 2024). NPs, comprising pieces smaller than 100 nm, represent an emerging health threat due to their inherent chemical composition or ability to absorb and transport other harmful substances. These potential dangers can be categorized into three main types: physical, chemical, and biological (Fontes et al., 2024). It should be noted that research on NPs is taking the first steps and the degradation processes and rates of MPs to NPs are not yet clear due to the limitation of technology.

In previous in vitro studies, we demonstrated that NPs affect cellular functions (Basini et al., 2022, 2023), thus representing a potential threat for reproductive function (Basini et al., 2021a). Therefore, this present research has been undertaken to expand knowledge on NPs effects using ovarian translational model represented by luteal and endothelial cells isolated from swine corpus luteum (Basini et al., 2014; Basini et al., 2021b).

Collected data show that metabolic activity, measured by ATP production, appear to be unaffected by NPs in luteal cells while increases in endothelial cells isolated from corpus luteum. Interestingly, recent studies agree with our present findings: in particular, results obtained in luteal cells agree with those in granulosa cells (Basini et al., 2021a) and data in endothelial cells are similar to those collected using aortic endothelial cell line (Basini et al., 2023). In general, our results differ from reported evidence showing a reduction in ATP levels, mainly attributable to mitochondrial damage, already documented in human embryonic cells (Li et al., 2023) and zebrafish (Woo et al., 2023). The reasons for these discrepancies are not clear at present and further investigation is required. Our present data show that cell proliferation is unaffected by NPs in endothelial cells, as reported in our previous study on aortic endothelial cells (Basini et al., 2023). Contrarily, cell proliferation is increased in luteal cells treated with NPs. In general, it should be noted that luteal cells, as they are differentiated, show lower mitotic activity compared with other cell types. However, in some animals like pigs and sheep, luteal cells retain their ability to proliferate (Murphy, 2000; Mlyczyńska et al., 2022). It should be noted that our isolation method guarantees the culture of a mixed population of large and small luteal cells. We think that the critical effect of NPs act to disrupt this low proliferation rate. Further studies are need in order to clarify the transduction mechanisms involved. Interestingly, our present findings agree with previous research on ovarian cells both in vitro (Basini et al., 2021a) and in vivo where it has been demonstrated that NPs interfere with the mitogen-activated protein kinase (MAPKs) pathway (Chen et al., 2024). (MAPK) signaling pathway is a highly conserved signal transduction pathway from yeast to human species, and is widely distributed in various eukaryotic cells. In almost all species studied over the past three decades, this signaling pathway plays a crucial role in the regulation of proliferation of female reproductive cells (Fan et al., 2012). Interestingly, it has been documented that reactive oxygen species (ROS) activate MAPKs thus stimulating cell proliferation (Lin et al., 2019).

Reactive oxygen species are important cellular messengers, mainly at the mitochondrial level during the process of cellular respiration. They support and assist in the homeostatic control of physiological and metabolic functions, such as cellular proliferation and differentiation, and are rapidly eliminated by detoxification systems such as enzymes, scavenger molecules and antioxidants. In agreement with our previous findings (Basini et al., 2021a, 2022, 2023), in both luteal and endothelial cells redox status appears to be disrupted by NPs. On the other hand, changes in ROS production can cause severe cell problems. In fact, a decrease can impair proliferation, stem cell differentiation as well as prevent the immune response activation, leading to immunosuppression. On the contrary, an increased production of ROS could enhance the release of proinflammatory cytokines and proliferation, as found in neoplastic cells (Mittler, 2017).

The results of our report also show that in luteal cells, subjected to treatment with NPs, progesterone (P4) levels significantly decreased. This result is supported by previous data which demonstrate that NPs can interfere with the production of hormones. A recent study (Basini et al., 2021a) documented a reduction in progesterone levels in sow granulosa cells treated with NPs; on the contrary, an in vivo study on female mice showed an increase in serum progesterone levels in cells subjected to NPs (Scsukova et al., 2017). In a study carried out on females of *Oryzias melastigma* it emerged that exposure to polystyrene NPs resulted in down-regulation in the expression of genes coding for 11β-hydroxysteroid dehydrogenase (11βHSD), steroidogenic acute regulatory protein (StAR) and cytochrome P450 17A1, i.e. for enzymes involved in the production of steroid hormones (Wang et al., 2019).

The formation of the corpus luteum and its maintenance are closely associated with angiogenesis. It has been demonstrated that high levels of ROS and NO, in addition to increasing oxidative stress and consequent cellular damage, are also capable of impairing the angiogenic processes homeostasis (Basini et al., 2016). It should be noted that also luteal cells express NOS (Vega et al., 1998; Tao et al., 2004). NO production by luteal cells has been detected also in our previous studies (Basini et al., 2021b; Dodi et al., 2021)

In vitro studies, using immortalized human cerebral microvascular endothelial cells, have demonstrated that NPs can be internalized into cells causing production of ROS, nuclear factor kappa-B (NF-kB), secretion of tumour necrosis factors α (TNF -α) as well as cell death (Shan et al., 2022). In agreement with various experimental evidence in the present study we showed that in endothelial cells the treatment with NPs induced an increase of free radical production, in association with an increase of SOD enzyme activity as well as of non-enzymatic antioxidant activity. These changes would likely represent a possible cell defence mechanism in controlling high concentrations of these compounds.

In the present study, we also quantified the production of VEGF by endothelial cells, i.e. the main angiogenic factor which acts mainly stimulating cell migration and increasing vascular permeability (Eelen et al., 2020). VEGF can be also produced by swine luteal cells as already demonstrated by other authors (Rytelewska et al., 2021; Bharati et al., 2024). Therefore, we are sought also to explore this aspect in further studies. Our data indicate that NPs treatment induces a significant increase in VEGF levels as already observed in aortic endothelial cell line (Basini et al., 2023). Interestingly, a study by Dai et al. (2023) in Zebrafish demonstrated an impairment of VEGF signalling mechanisms.

Furthermore, we sought to verify the nature of the NPs accumulation in endothelial cells through fluorescence microscopy. A significant increase of the NPs load, calculated as the (NPs Area/Endothelial Cell Area) ratio, was reported from the lowest concentration tested, 5 μg/mL, to 25 μg/mL and 75 μg/mL (Fig. 7), demonstrating a dose-dependent accumulation of NPs in endothelial cells. These results were consistent with our previous study conducted on endothelial cells isolated from swine aorta (Basini et al., 2023). In endothelial cells treated with NPs we observed the accumulation of NPs wrapped around F-actin filaments that localized in between the extracellular and the intracellular space (Fig. S1), likely evidencing the occurrence of NPs adhesion to the cell surface and internalization. A recent study reported that NPs of 100 nm of diameter, the same of the NPs used in the present work, were able not only to adhere to human umbilical vein endothelial cells, but also to be taken up by cells and aggregate into the cytoplasm (Lu et al., 2022). Thus, to further investigate the possible internalization of NPs, we combined the imaging of fluorescent NPs and fluorescently labelled lysosomes (LAMP-1) in cells exposed to 5 μg/mL of NPs. The z-dimensional co-localization with lysosomes confirmed the cytosolic localization of NPs, as shown in orthogonal projections and 3D reconstructions in Fig. 8. Even if the localization of NPs within the lysosomes was reported in other cell types, like intestinal epithelial cells and macrophages (Brandts et al., 2023; Xu et al., 2021; Khan et al., 2023), we didn't observe a distinct overlap between NPs and LAMP-1 fluorescent signals, suggesting that NPs were internalized, but were not included into LAMP-1 positive lysosomes. Liu and colleagues (2021) demonstrated that NPs between 50 and 500 nm of diameter could passively penetrate the cytoplasmic membrane due to hydrophobic interactions and Van deer Waals' forces and initially distribute in the cytoplasm and not in lysosomes (Liu et al., 2021). Since we observed the presence of NPs at the cytosolic level, but not within lysosomes, we speculated that passive internalization could be one of the possible mechanisms behind the observed NPs up-take. Moreover, we observed the presence of extracellular NPs that did not co-localized in z-dimension with lysosomes (Fig. S2), likely suggesting their adhesion to the cell surface. Even if NPs internalization was demonstrated through qualitative analysis by fluorescence microscopy, further investigations are needed to define the precise uptake mechanisms and the consequent organelle localization of NPs in microvascular endothelial cells specific of reproductive organ.

5. Conclusions

The present study adds new evidence about the effects of exposure to NPs on both endocrine and endothelial cells of the reproductive system. The data collected show an increase of ROS production, in the antioxidant defence, a significant decrease in the production of progesterone, a fundamental hormone in maintaining correct reproductive function and an increased vascular endothelial growth factor (VEGF A) level, the main angiogenic factor. Furthermore, through fluorescence microscopy it was possible to quantify a dose-dependent accumulation of NPs in endothelial cells specific of the corpus luteum, occurred through adhesion and internalization. Therefore, the results obtained indicate that NPs can impair reproductive functionality and angiogenic mechanisms. Further studies are needed to unravel the molecular machineries responsible for the effects we have described.

CRediT authorship contribution statement

Francesca Zappavigna: Formal analysis, Data curation. **Giuseppina Basini:** Writing – review & editing, Writing – original draft, Supervision, Project administration, Methodology, Conceptualization. **Simona Bussolati:** Methodology, Formal analysis, Data curation. **Simone Bertini:** Writing – review & editing, Project administration, Funding acquisition. **Stefano Grolli:** Writing – review & editing, Writing – original draft. **Roberto Ramoni:** Writing – review & editing, Writing – original draft. **Francesca Grasselli:** Writing – review & editing, Writing – original draft, Conceptualization. **Fausto Quintavalla:** Writing – review & editing, Writing – original draft. **Erika Scaltriti:** Writing – review & editing, Writing – original draft, Software, Formal analysis. **Melissa Berni:** Writing – review & editing, Writing – original draft, Software, Investigation, Formal analysis.

Declaration of Competing Interest

The authors declare that they have no known competing financial interests or personal relationships that could have appeared to influence the work reported in this paper.

Data availability

Data will be made available on request.

Acknowledgements

This research was supported by the Program "FIL-Quota Incentivante" of University of Parma and co-sponsored by Fondazione Cariparma.

Appendix A. Supporting information

Supplementary data associated with this article can be found in the online version at doi:10.1016/j.etap.2024.104503.

References

Akins, E.L., Morrissette, M.C., 1968. Gross ovarian changes during estrous cycle of swine. Am. J. Vet. Res *29*, 1953–1957.
Ali, S.S., Elsamahy, T., Al-Tohamy, R., Zhu, D., Mahmoud, Y.A., Koutra, E., Metwally, M. A., Kornaros, M., Sun, J., 2021. Plastic wastes biodegradation: mechanisms, challenges and future prospects. Sci. Total. Environ. *780*, 146590.
Athulya, P.A., Waychal, Y., Rodriguez-Seijo, A., Devalla, S., Doss, C.G.P., Chandrasekaran, N., 2024. Microplastic interactions in the agroecosystems: methodological advances and limitations in quantifying microplastics from agricultural soil. Environ. Geochem. Health *46*, 85.
Babalola, G.O., Shapiro, B.H., 1988. Correlation of follicular steroid hormone profiles with ovarian cyclicity in sows. J. Reprod. Fertil. *84*, 79–87.
Barboni, B., Turriani, M., Galeati, G., Spinaci, M., Bacci, M.L., Forni, M., Mattioli, M., 2000. Vascular endothelial growth factor production in growing pig antral follicles. Biol. Reprod. *63*, 858–864.
Basini, G., Bussolati, S., Baioni, L., Grasselli, F., 2009a. Gossypol, a polyphenolic aldehyde from cotton plant, interferes with swine granulosa cell function. Domest. Anim. Endocrinol. *37*, 30–36.
Basini, G., Santini, S.E., Bussolati, S., Grasselli, F., 2009b. The phytoestrogen Quercetin Impairs Steroidogenesis and Angiogenesis in swine granulosa cells in vitro. J. Biomed. Biotech. *2009*, 1–8.
Basini, G., Bussolati, S., Santini, S.E., Grasselli, F., 2010. The impact of the phyto-oestrogen genistein on swine granulosa cell function. J. Anim. Physiol. Anim. Nutr. (Berl.) *94*, e374–e382.
Basini, G., Falasconi, I., Bussolati, S., Grolli, S., Ramoni, R., Grasselli, F., 2014. Isolation of endothelial cells and pericytes from swine corpus luteum. Domest. Anim. Endocrinol. *48*, 100–109.
Basini, G., Falasconi, I., Bussolati, S., Grolli, S., Di Lecce, R., Grasselli, F., 2016. Swine granulosa cells show typical endothelial cell characteristics. Reprod. Sci. *23*, 630–637.
Basini, G., Bussolati, S., Ciccimarra, R., Grasselli, F., 2017. Melatonin potentially acts directly on swine ovary by modulating granulosa cell function and angiogenesis. Reprod. Fertil. Dev. *29*, 2305–2312.
Basini, G., Ciccimarra, R., Bussolati, S., Grolli, S., Ragionieri, L., Ravanetti, F., Botti, M., Gazza, F., Cacchioli, A., Di Lecce, R., Cantoni, A.M., Grasselli, F., 2018. Orexin A in swine corpus luteum. Domest. Anim. Endocrinol. *64*, 38–48.
Basini, G., Bussolati, S., Bertini, S., Quintavalla, F., Grasselli, F., 2021. B. Evaluation of Triclosan Effects on Cultured Swine Luteal Cells. Anim. (Basel) *11*, 606.
Basini, G., Bussolati, S., Andriani, L., Grolli, S., Ramoni, R., Bertini, S., Iemmi, T., Menozzi, A., Berni, P., Grasselli, F., 2021. A. Nanoplastics impair in vitro swine granulosa cell functions. Domest. Anim. Endocrinol. *76*, 106611.
Basini, G., Bussolati, S., Andriani, L., Grolli, S., Bertini, S., Iemmi, T., Menozzi, A., Quintavalla, F., Ramoni, R., Serventi, P., Grasselli, F., 2022. The effects of nanoplastics on adipose stromal cells from swine tissues. Domest. Anim. Endocrinol. *81*, 106747.
Basini, G., Grolli, S., Bertini, S., Bussolati, S., Berni, M., Berni, P., Ramoni, R., Scaltriti, E., Quintavalla, F., Grasselli, F., 2023. Nanoplastics induced oxidative stress and VEGF production in aortic endothelial cells. Environ. Toxicol. Pharmacol. *104*, 104294.
Basini, G., Bussolati, S., Grolli, S., Berni, P., Grasselli, F., 2024. Are the new phthalates safe? Evaluation of Diisononilphtalate (DINP) effects in porcine ovarian cell cultures. Environ. Toxicol. Pharmacol. 106, 104384.
Berni, M., Pongolini, S., Tambassi, M., 2022. Automated Analysis of Intracellular Phenotypes of Salmonella using ImageJ. J. Vis. Exp. (*186*) https://doi.org/10.3791/64263.
Bharati, J., Kumar, S., Mohan, N.H., Pegu, S.R., Borah, S., Gupta, V.K., Sarkar, M., 2024. CRISPR/Cas genome editing revealed non-angiogenic role of VEGFA gene in porcine luteal cells: a preliminary report. Mol. Biol. Rep. *51*, 195.
Brandts, I., Solà, R., Garcia-Ordoñez, M., Gella, A., Quintana, A., Martin, B., Esteve-Codina, A., Telesab, M., Roher, N., 2023. Polystyrene nanoplastics target lysosomes interfering with lipid metabolism through the PPAR system and affecting macrophage functionalization. Environ. Sci. Nano *10*, 2245.
Chen, G., Shan, H., Xiong, S., Zhao, Y., van Gestel, C.A.M., Qiu, H., Wang, Y., 2024. Polystyrene nanoparticle exposure accelerates ovarian cancer development in mice by altering the tumor microenvironment. Sci. Total Environ. *906*, 167592.
Dai, L., Luo, J., Feng, M., Wang, M., Zhang, J., Cao, X., Yang, X., Li, J., 2023. Nanoplastics exposure induces vascular malformation by interfering with the VEGFA/VEGFR pathway in zebrafish (Danio rerio). Chemosphere *312*, 137360.
Dodi, A., Bussolati, S., Grolli, S., Grasselli, F., Di Lecce, R., Basini, G., 2021. Melatonin modulates swine luteal and adipose stromal cell functions. Reprod. Fertil. Dev. *33*, 198–208.
Dong, X., Liu, X., Hou, Q., Wang, Z., 2023. From natural environment to animal tissues: A review of microplastics (nanoplastics) translocation and hazards studies. Sci. Total Environ. *855*, 158686.
Eelen, G., Treps, L., Li, X., Carmeliet, P., 2020. Basic and therapeutic aspects of angiogenesis updated. Circ. Res. *127*, 310–329.
Ekanayake, A., Rajapaksha, A.U., Hewawasam, C., Anand, U., Bontempi, E., Kurwadkar, S., Biswas, J.K., Vithanage, M., 2023. Environmental challenges of

COVID-19 pandemic: resilience and sustainability - A review. Environ. Res. *216*, 114496.

Fan, H.Y., Liu, Z., Mullany, L.K., Richards, J.S., 2012. Consequences of RAS and MAPK activation in the ovary: the good, the bad and the ugly. Mol. Cell. Endocrinol. *356*, 74–79.

Ferreira, O., Barboza, L.G.A., Rudnitskaya, A., Moreirinha, C., Vieira, L.R., Botelho, M.J., Vale, C., Fernandes, J.O., Cunha, S., Guilhermino, L., 2023. Microplastics in marine mussels, biological effects and human risk of intake: A case study in a multi-stressor environment. Mar. Pollut. Bull. *197*, 115704.

Fontes, B.L.M., de Souza, E., Souza, L.C., da Silva de Oliveira, A.P.S., da Fonseca, R.N., Neto, M.P.C., Pinheiro, C.R., 2024. The possible impacts of nano and microplastics on human health: lessons from experimental models across multiple organs. J. Toxicol. Environ. Health B Crit. Rev. *27*, 153–187.

Gospodarowicz, D., Gospodarowicz, F., 1972. A technique for the isolation of bovine luteal cells and its application to metabolic studies of luteal cells in vitro. Endocrinology *90*, 1427–1434.

Gregoraszczuk, E.L., Oblonczyk, K., 1996. Effect of a specific aromatase inhibitor on oestradiol secretion by porcine corpora lutea at various stages of the luteal phase. Reprod. Nutr. Dev. *36*, 65–72.

Heidbreder, L.M., Bablok, I., Drews, S., Menzel, C., 2019. Tackling the plastic problem: A review on perceptions, behaviors, and interventions. Sci. Total. Environ. *668*, 1077–1093.

Hong, Y., Wu, S., Wei, G., 2023. Adverse effects of microplastics and nanoplastics on the reproductive system: A comprehensive review of fertility and potential harmful interactions. Sci. Total Environ. *903*, 166258.

Huang, J., Zou, L., Bao, M., Feng, Q., Xia, W., Zhu, C., 2023. Toxicity of polystyrene nanoparticles for mouse ovary and cultured human granulosa cells. Ecotoxicol. Environ. Saf. *249*, 114371.

Jeong, J., Im, J., Choi, J., 2024. Integrating aggregate exposure pathway and adverse outcome pathway for micro/nanoplastics: A review on exposure, toxicokinetics, and toxicity studies. Ecotoxicol. Environ. Saf. *272*, 116022.

Junaid, M., Hamid, N., Liu, S., Abbas, Z., Imran, M., Haider, M.R., Wang, B., Chen, G., Khan, H.K., Yue, Q., Xu, N., Wang, J., 2024. Interactive impacts of photoaged micro (nano)plastics and co-occurring chemicals in the environment. Sci. Total Environ. *927*, 172213.

Khan, A., Jia, Z., 2023. Recent insights into uptake, toxicity, and molecular targets of microplastics and nanoplastics relevant to human health impacts. iScience 26, 106061.

Lee, S.E., Yoon, H.K., Kim, D.Y., Jeong, T.S., Park, Y.S., 2024. An emerging role of micro- and nanoplastics in vascular diseases. Life (Basel) *14*, 255.

Lehner, R., Weder, C., Petri-Fink, A., Rothen-Rutishauser, B., 2019. Emergence of Nanoplastic in the Environment and Possible Impact on Human Health. Environ. Sci. Technol. *53*, 1748–1765.

Leso, V., Battistini, B., Vetrani, I., Reppuccia, L., Fedele, M., Ruggieri, F., Bocca, B., Iavicoli, I., 2023. The endocrine disrupting effects of nanoplastic exposure: A systematic review. Toxicol. Ind. Health *39*, 613–629.

Leung, P.C.K., Adashi, E.Y., 2018. The Ovary. Elsevier.

Li, Y., Li, Y., Li, J., Song, Z., Zhang, C., Guan, B., 2023. Toxicity of polystyrene nanoplastics to human embryonic kidney cells and human normal liver cells: Effect of particle size and Pb2+ enrichment. Chemosphere *328*, 138545.

Lin, W., Jiang, R., Hu, S., Xiao, X., Wu, J., Wei, S., Xiong, Y., Ouyang, G., 2019. Investigating the toxicities of different functionalized polystyrene nanoplastics on Daphnia magna. Ecotoxitol. Environ. Saf. *180*, 509–516.

Liu, L., Xu, K., Zhang, B., Ye, Y., Zhang, Q., Jiang, W., 2021. Cellular internalization and release of polystyrene microplastics and nanoplastics. Sci. Total Environ. *779*, 146523.

Liza, A.A., Ashrafy, A., Islam, M.N., Billah, M.M., Arafat, S.T., Rahman, M.M., Karim, M. R., Hasan, M.M., Promie, A.R., Rahman, S.M., 2024. Microplastic pollution: a review of techniques to identify microplastics and their threats to the aquatic ecosystem. Environ. Monit. Assess. *196*, 285.

Lu, Y.Y., Li, H., Ren, H., Zhang, X., Huang, F., Zhang, D., Huang, Q., Zhang, X., 2022. Size-dependent effects of polystyrene nanoplastics on autophagy response in human umbilical vein endothelial cells. J. Hazard Mater. *421*, 126770.

Malafeev, K.V., Apicella, A., Incarnato, L., Scarfato, P., 2023. Understanding the Impact of Biodegradable Microplastics on Living Organisms Entering the Food Chain: A Review. Polym. (Basel) *15*, 3680.

McDonald, L.E., 1975. Veterinary Endocrinology and Reproduction, 2nd edn. Lea & Febiger, Philadelphia, pp. 283–285.

Milne, M.H., De Frond, H., Rochman, C.M., Mallos, N.J., Leonard, G.H., Baechler, B.R., 2024. Exposure of U.S. adults to microplastics from commonly-consumed proteins. Environ. Pollut. *343*, 123233.

Mittler, R., 2017. ROS Are Good. Trends Plant Sci. *22*, 11–19.

Mlyczyńska, E., Kieżun, M., Kurowska, P., Dawid, M., Pich, K., Respekta, N., Daudon, M., Rytelewska, E., Dobrzyń, K., Kamińska, B., Kamiński, T., Smolińska, N., Dupont, J., Rak, A., 2022. New Aspects of Corpus Luteum Regulation in Physiological and Pathological Conditions: Involvement of Adipokines and Neuropeptides. Cells *11*, 957.

Murphy, B.D. 2000. Models of luteinization. Biol. Reprod. 63, 2–11.

Nitkiewicz, A., Smolinska, N., Przała, J., Kaminski, T., 2010. Expression of orexin receptors 1 (OX1R) and 2 (OX2R) in the porcine ovary during the oestrous cycle. Regul. Pept. *165*, 186–190.

PlasticsEurope. Plastics – The Fast Facts 2023 https://plasticseurope.org/knowledge-hub/plastics-the-fast-facts-2023/.

Robinson, R.S., Woad, K.J., Hammond, A.J., Laird, M., Hunter, M.G., Mann, G.E., 2009. Angiogenesis and vascular function in the ovary. Reproduction *138*, 869–881.

Rytelewska, E., Kiezun, M., Zaobidna, E., Gudelska, M., Kisielewska, K., Dobrzyn, K., Kaminski, T., Smolinska, N., 2021. Chemerin as a modulator of angiogenesis and apoptosis processes in the corpus luteum of pigs: an in vitro study†. Biol. Reprod. *105*, 1002–1015.

Sangale, M.K., Shahnawaz, M., Ade, A.B., 2019. Potential of fungi isolated from the dumping sites mangrove rhizosphere soil to degrade polythene. Sci. Rep. *9*, 5390.

Schindelin, J., Arganda-Carreras, I., Frise, E., Kaynig, V., Longair, M., Pietzsch, T., Preibisch, S., Rueden, C., Saalfeld, S., Schmid, B., Tinevez, J.Y., White, D.J., Hartenstein, V., Eliceiri, K., Tomancak, P., Cardona, A., 2012. Fiji: an open-source platform for biological-image analysis. Nat. Methods *9*, 676–682.

Scsukova, S., Bujnakova, M.A., Kiss, A., Rollerova, E., 2017. Adverse eff ects of polymeric nanoparticle poly(ethylene glycol)- block-polylactide methyl ether (PEG-b-PLA) on steroid hormone secretion by porcine granulosa cells. Endocr. Regul. *51*, 96–104.

Sewwandi, M., Wijesekara, H., Rajapaksha, A.U., Soysa, S., Vithanage, M., 2023. Microplastics and plastics-associated contaminants in food and beverages; Global trends, concentrations, and human exposure. Environ. Pollut. *317*, 120747.

Shan, S., Zhang, Y., Zhao, H., Zeng, T., Zhao, X., 2022. Polystyrene nanoplastics penetrate across the blood-brain barrier and induce activation of microglia in the brain of mice. Chemosphere *298*, 134261.

Shen, M., Zhang, Y., Zhu, Y., Song, B., Zeng, G., Hu, D., Wen, X., Ren, X., 2019. Recent advances in toxicological research of nanoplastics in the environment: A review. Environ. Pollut. *252*, 511–521.

Shiwakoti, S., Ko, J.Y., Gong, D., Lee, J.H., Adhikari, R., Gwak, Y., Park, S.H., Jun Choi, I., Schini-Kerth, V.B., Kang, K.W., Oak, M.H., 2022. Effects of polystyrene nanoplastics on endothelium senescence and its underlying mechanism. Environ. Int. *164*, 107248.

Spanel-Borowski, K., van der Bosch, J., 1990. Different phenotyes of cultured microvessel endothelial cells obtained from bovine corpus luteum. Cell Tissue Res *261*, 35–47.

Sridharan, S., Kumar, M., Singh, L., Bolan, N.S., Saha, M., 2021. Microplastics as an emerging source of particulate air pollution: A critical review. J. Hazard Mater. *418*, 126245.

Tao, Y., Fu, Z., Zhang, M., Xia, G., Yang, J., Xie, H., 2004. Immunohistochemical localization of inducible and endothelial nitric oxide synthase in porcine ovaries and effects of NO on antrum formation and oocyte meiotic maturation. Mol. Cell. Endocrinol. *222*, 93–103.

Vega, M., Johnson, M.C., Díaz, H.A., Urrutia, L.R., Troncoso, J.L., Devoto, L., 1998. Regulation of human luteal steroidogenesis in vitro by nitric oxide. Endocrine 8, 185–191.

Wang, J., Li, Y., Lu, L., Zheng, M., Zhang, X., Tian, H., Wang, W., Ru, S., 2019. Polystyrene microplastics cause tissue damages, sex-specific reproductive disruption and transgenerational effects in marine medaka (Oryzias melastigma). Environ. Pollut. *254*, 113024.

Wei, W., Li, Y., Lee, M., Lin, S., Chen, C., Leong, D.T., Ding, F., Song, Y., Ke, P.C., 2022. Anionic nanoplastic exposure induces endothelial leakiness. Nat. Commun. *13*, 4757.

Woo, J.H., Seo, H.J., Lee, J.Y., Lee, I., Jeon, K., Kim, B., Lee, K., 2023. Polypropylene nanoplastic exposure leads to lung inflammation through p38-mediated NF-κB pathway due to mitochondrial damage. Part. Fibre Toxicol. *20*, 2.

Xu, D., Ma, Y., Han, X., Chen, Y., 2021. Systematic toxicity evaluation of polystyrene nanoplastics on mice and molecular mechanism investigation about their internalization into Caco-2 cells. J. Hazard Mater. *417*, 126092.

Zeng, L., Zhou, C., Xu, W., Huang, Y., Wang, W., Ma, Z., Huang, J., Li, J., Hu, L., Xue, Y., Luo, T., Zheng, L., 2023. The ovarian-related effects of polystyrene nanoplastics on human ovarian granulosa cells and female mice. Ecotoxicol. Environ. Saf. *257*, 114941.